

Evolution of disease transmission rate during the course of SARS-COV-2: Patterns and determinants

Jie Zhu

UNSW Sydney <https://orcid.org/0000-0002-1863-9262>

Blanca Gallego (✉ b.gallego@unsw.edu.au)

UNSW Sydney

Research Article

Keywords: Public Health Intervention, Stochastic Model, Epidemic Modelling

Posted Date: April 7th, 2021

DOI: <https://doi.org/10.21203/rs.3.rs-44647/v2>

License:   This work is licensed under a Creative Commons Attribution 4.0 International License.

[Read Full License](#)

Version of Record: A version of this preprint was published on May 26th, 2021. See the published version at <https://doi.org/10.1038/s41598-021-90347-8>.

Evolution of disease transmission during the course of SARS-COV-2: patterns and determinants

Jie Zhu, Blanca Gallego*

Centre for Big Data Research in Health, UNSW Sydney, Sydney, 2052, NSW, Australia

Abstract

Background

This has been the first time in recent history when extreme measures that have deep and wide impact on our economic and social systems, such as lock downs and border closings, have been adopted at a global scale. These measures have been taken in response to the severe acute respiratory syndrome coronavirus SARS-CoV-2 pandemic, declared a Public Health Emergency of International Concern on 30 January 2020. Epidemic models are being used by governments across the world to inform social distancing and other public health strategies to reduce the spread of the virus. These models, which vary widely in their complexity, simulate interventions by manipulating model parameters that control social mixing, healthcare provision and other behavioral and environmental processes of disease transmission and recovery. The validity of these parameters is challenged by the uncertainty of the impact on disease transmission from socio-economic factors and public health interventions. Although sensitivity of the models to small variations in parameters are often carried out, the forecasting accuracy of these models is rarely investigated during an outbreak.

Methods

We fitted a stochastic transmission model on reported cases, recoveries and deaths associated with the infection of SARS-CoV-2 across 101 countries that had adopted at least one social-distancing policy by 15 May 2020. The dynamics of disease transmission was represented in terms of the daily effective reproduction number (R_t). Countries were grouped according to their initial temporal R_t patterns using a hierarchical clustering algorithm. We then computed the time lagged cross correlation among the daily number of policies implemented (policy volume), the daily effective reproduction number, and the daily incidence counts for each country. Finally, we provided forecasts of incidence counts up to 30-days from the time of prediction for each country repeated over 230 daily rolling windows from 15 May to 31 Dec 2020. The forecasting accuracy of the model when R_t is updated every time a new prediction is made was compared with the accuracy using a static R_t .

Findings

We identified 5 groups of countries with distinct transmission patterns during the first 6 months of the pandemic. Early adoption of social distancing measures and a shorter gap between any two interventions were associated with a reduction on the duration of outbreaks (with correlation coefficients of -0.26 and 0.24 respectively). Sustained social distancing appeared to play a role in the prevention of the second transmission peak. By 15 May 2020, the average of the median R_t across examined countries had reduced from its peak of 20.5 (17.79, 23.20) to 1.3 (0.94, 1.74).

The time lagged cross correlation analysis revealed that increased policy volume was associated with lower future R_t (the negative correlation was minimized when R_t lagged the policy volume by 75 days), while a lower R_t was associated with lower future policy volume (the positive correlation was maximized when R_t led by 102 days). R_t led the daily incidence counts by 78 days, with lower incidence counts being associated with lower future policy volume (the positive correlation was maximized when counts led the volume by 135 days). On the other hand, higher policy volume was not associated with lower incidence counts within a lag of up to 180 days.

The outbreak prediction accuracy of the stochastic transmission model using dynamically updated R_t produced an average AUROC of 0.72 (0.708, 0.723) compared to 0.56 (0.555, 0.568) when R_t was kept constant. Prediction

accuracy declined with forecasting time.

Interpretation

Understanding the evolution of the daily effective reproduction number during an epidemic is an important complementary piece of information to reported daily counts, recoveries and deaths. This is because R_t provides an early signal of the efficacy of containment measures. Using updated R_t values produces significantly better predictions of future outbreaks. Our results found a substantial variation in the effect of early public health interventions on the evolution of R_t over time and across countries, which could not be explained solely by the timing and number of the adopted interventions. This suggests that further knowledge about the idiosyncrasy of the implementation and effectiveness thereof is required. Although sustained containment measures have successfully lowered growth rate of disease transmission, more than half of the studied countries failed to maintain an effective reproduction number close to or below 1. This resulted in continued growth in reported cases.

1 Introduction

Mathematical and computational models of disease outbreaks are used to generate knowledge about the biological, behavioral and environmental processes of disease transmission, as well as to forecast disease progression. Public health responders rely on insights provided by these models to guide disease control strategies.¹ As an example, in mid March 2020, the British government changed its SARS-CoV-2 response policy following a brief on simulation results from Ferguson et al.², which indicated an unacceptable forecasted number of deaths in the absence of more stringent control measures.

Different models have been applied to model the spatial and temporal dynamics of SARS-CoV-2 (see the review study³). They range from simple deterministic population-based models⁴⁻⁶, that assume uniform mixing, to complex agent-based models^{2,7} in which individuals defined by different attributes related to their susceptibility, infectiousness and social interactions transmit the pathogen to each other given rise to heterogeneous transmission patterns.

Irrespective of their complexity, the accuracy of these models is constrained by the validity of the epidemiological parameters that underpin them. For example, the model parameters controlling the risk of infection together with the social contact between infectious and susceptible individuals determine the transmission rate, which in turns influences the peak and duration of the epidemics. By manipulating these parameters, modelers can represent the impact of public health measures such as social distancing (lowering the contact rate) or wearing protective masks (lowering the risk of infection).

This study evaluates the effectiveness of initial public health interventions globally by estimating the effective reproduction number (the expected number of secondary infections resulting from an infectious individual) on a daily basis and highlights the importance of using updated reproduction numbers for outbreak forecast. In section 2, we describe the methods. In section 3, we first present the patterns of initial public health interventions and effective reproduction numbers for a fixed temporal window across countries. Then we look into temporal patterns of number of public health interventions, effective reproduction number and incidence counts using a time lagged cross correlation analysis. Lastly, future outbreaks are predicted to illustrate how the currency of epidemiological parameters can influence the forecasting of expected infection counts. We end with a discussion.

*Corresponding author.

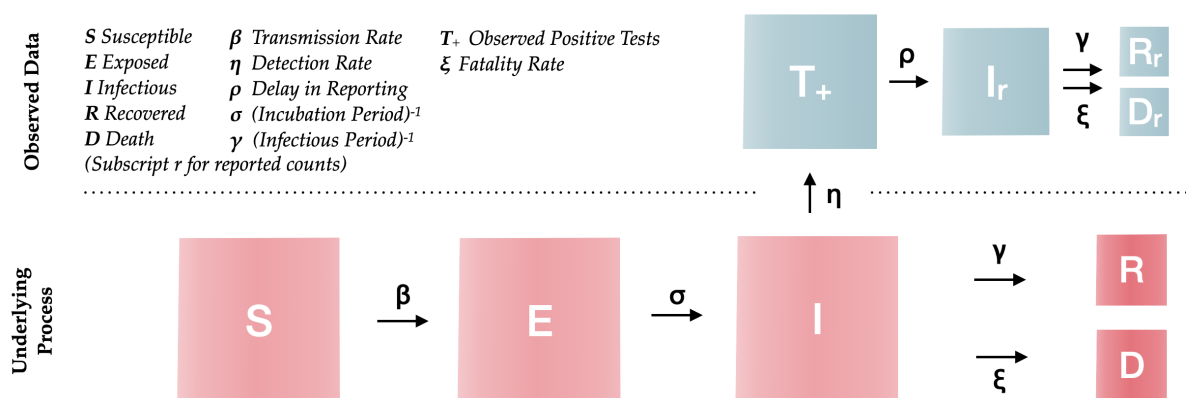
Email addresses: elliott.zhu@unsw.edu.au (Jie Zhu), b.gallego@unsw.edu.au (Blanca Gallego)

2 Method

2.1 Data Sources

By 15 May 2020, there were 188 countries with recorded incidence of the infection of SARS-COV-2 and 101 of them had implemented at least one public health intervention to contain the spread of the virus and had at least one death⁸. We modeled the transmission dynamics of SARS-COV-2 between 22 Jan to 15 May 2020 via fitting a stochastic SEIRD model⁹ (illustrated in Figure 1) to three available time series: 1) Daily number of incident cases, 2) Daily number of deaths, and 3) Daily number of recoveries, as recorded, for each country, by the Johns Hopkins Coronavirus Resource Center¹⁰.

Figure 1. Simulation model structure.



The population is divided into the following five classes: susceptible, exposed (non-infectious and asymptomatic), infectious (asymptomatic and symptomatic), removed (i.e., isolated, recovered, or otherwise non-infectious) and dead. The reported data is modeled with four classes: observed positive tests, reported infections, removed and deaths.

To monitor public health interventions, we captured government stringent policies using the Oxford Covid-19 government response tracker⁸, which contains 17 policies organized into three groups: containment and closure policies, economic policies and health system policies. We explored 12 of these policies, namely those that have a more immediate and direct impact on individual's lifestyle and well-being. Social distancing policies (including travel policies) were further classified into two levels depending on whether the government took a recommended or required stance; and international travel controls were divided into four levels: 1) screening arrivals, 2) quarantine arrivals from some or all regions, 3) ban arrivals from some regions, and 4) ban on all regions or total border closure.

2.2 Epidemic simulation model and analysis of transmission patterns

We built an extended version of a SEIRD model that included transitions between reporting states and disease states in order to account for delays in reporting (Figure 1). The model incorporates uncertainty in reported counts by explicitly modeling a Poisson process of daily reported infectious, recovered and dead counts, as well as infectious individuals detected. Following previous literature^{11,12}, the mean incubation period was assumed to be Erlang distributed with mean 5.2 days (SD 3.7)¹³ and the mean infectious period was assumed to be Erlang distributed with mean 2.9 days (2.1).¹² A sensitivity analysis of these two parameters on the prediction performance of SEIRD model was performed and can be found in the supplementary material.

For each country k , the daily transmission rate ($\beta_{t,k}$) and fatality rate ($\xi_{t,k}$) were modeled as a geometric random walk process, and sequential Monte Carlo simulation was used to infer the daily reproduction number, $R_{t,k}$ (defined as the transmission rate over the assumed incubation period $\beta_{t,k}/\gamma$), as well as the daily fatality rate. The remaining unknown parameters were estimated via grid search using the maximum likelihood method. In each country, we

assumed the outbreak started from the first infectious case and the entire population was initially susceptible. Further details on the model can be found in the supplementary material.

We summarized the patterns of estimated effective reproduction number using smoothed time series of $R_{t,k}$ generated by the Savitzky-Golay finite impulse response¹⁴ (FIR) filter. We compared hierarchical clustering from three algorithms: the WPGMA (Weighted Pair Group Method with Arithmetic Mean), the Centroid linkage algorithm and the Ward variance minimization method.

Our study uses descriptive statistics to analyze the patterns of $R_{t,k}$ and early public health interventions before 15 May 2020. We characterized time series of $R_{t,k}$ by their peak and the duration thereof. In particular, we define the following metrics, where we drop the country index k for simplicity:

- R_t peak, defined as the day of observing the maximum of the estimated effective reproduction number curve before 15 May 2020;
- R_t peak duration, defined as the time it takes R_t to reduce to 50% of R_t peak;

We related these metrics with three metrics captured over 8 social distancing policies:

- Policy timing (days from onset), defined as days taken from the outbreak onset to the intervention;
- Policy volume, which refers to the number of interventions applied; and
- Policy gap, defined as the average number of days between any two policies.

In addition to the static analysis of early control measures and R_t patterns at the beginning of the pandemic, we conducted a time lagged cross correlation (TLCC) analysis of the daily policy volume, the daily effective reproduction number, and the daily incidence counts from the first case detected in each country until the end of 2020. Please refer to the supplement for implementation detail.

Finally, we measured the prediction accuracy of our stochastic SEIRD compartment model up to 30 days from the time of prediction over 230 daily rolling windows ($j \in \{1, 2, \dots, 230\}$) from 15 May 2020 to 31 Dec 2020. An outbreak associated with prediction j in country k was defined as:

$$Y_{k,j} = E_{k,j}/C_{k,j} > q, q \in [1, 3], Y_{k,j} \in \{0, 1\}$$

where $E_{k,j}$ is the cumulative count of cases at the end of the j th window, $C_{k,j}$ is the cumulative count of cases at the beginning of the j th window and q is the growth rate threshold. There is an outbreak if $Y_{k,j} = 1$. Similarly, the predicted outcome is given by

$$\hat{Y}_{k,j} = \hat{E}_{k,j}/\hat{C}_{k,j} > q, \hat{Y}_{k,j} \in \{0, 1\}$$

To quantify the impact of the currency of transmission parameters on outbreak predictions, we estimated future incidence counts for each j and k in two ways: (1) with a constant $R_{t,k}$ defined as the average $R_{t,k}$ over the last five days at the beginning of the forecasting study, that is from the 11th to the 15th of May 2020, and (2) with a dynamic $R_{t,k}$ that is updated daily as the average $R_{t,k}$ over the last five-days before the time of prediction.

An area under the receiver operating characteristic curve (AUROC) over the range of q was estimated using true positive and false positive rates.¹⁵ The AUROC from the model with a dynamic effective reproduction number was compared against that with a static effective reproduction number.

Table 1. Key descriptive statistics across clusters as at 15 May 2020.

	Metric	Cluster 1 (12)	Cluster 2 (20)	Cluster 3 (4)	Cluster 4 (51)	Cluster 5 (14)
R_t Peak	Duration (days)	9.9 (2.14)	6.6 (1.38)	6 (1.52)	4.4 (0.56)	3.7 (1.12)
	Days from the outbreak	14.7 (5.10)/45.7 (8.62)	21.8 (9.21)	30.3 (3.08)	25.5 (5.80)	18.1 (6.07)
R_t	Mean	2.3 (0.20)	2.7 (0.30)	2.9 (0.30)	2.6 (0.22)	4.8 (1.36)
	SD	1.4 (0.14)	2.5 (0.49)	2.8 (0.66)	3.1 (0.75)	12.7 (4.06)
Policy	Gap (days)	13.1 (3.97)	7.1 (2.04)	8.7 (5.75)	7.8 (1.93)	9.9 (2.59)
	Volume (number)	6.8 (0.50)	7.3 (0.62)	5.8 (2.63)	7.1 (0.34)	7.1 (0.45)
	Timing (days from onset)	41.8 (3.78)	12.9 (2.39)	34.5 (8.96)	11.2 (2.78)	7.9 (1.20)
Reported Statistics	Tests/'000	21.5 (8.95)	19.1 (10.93)	35.7 (13.1)	10.5 (6.5)	10.2 (7.21)
	Reported deaths/'000	0.13 (0.10)	0.08 (0.06)	0.56 (0.17)	0.01 (0.001)	0.13 (0.17)
Reported Statistics	Reported infections/'000	1.5 (0.80)	1.7 (1.11)	4.1 (1.00)	0.9 (0.49)	2.1 (2.61)
	Death/Infection	0.06 (0.03)	0.04 (0.01)	0.14 (0.02)	0.03 (0.001)	0.05 (0.02)

This table displays selected descriptive statistics from 101 selected countries at the beginning of the pandemic up to 15 May 2020. The first section (as indicated by the solid horizontal lines) records the pattern of estimated daily reproduction number. Only cluster 1 is characterized by countries having two peaks of similar levels in their daily reproduction numbers. The second section summarizes the pattern of 8 social distancing policies. The last section records the average number of observed tests, reported deaths, reported infections per thousand population and reported deaths per infection. We averaged these values across countries in each cluster and recorded their sample standard error times the 95% confidence level value in brackets. For a detailed description of each examined policy the reader is referred to the supplementary material.

3 Results

3.1 Patterns of initial public health interventions and effective reproduction number

Our three clustering algorithms identified the same 5 distinct patterns of R_t at the second level of the hierarchy tree (results from WPGMA are provided in the supplementary material). Patterns of R_t were summarized by their peak duration, days to peak, mean and standard deviation. Table 1 shows these values for each cluster, together with the timing, volume and gap of public health interventions, as well as the number of infections, deaths and tests. A visual illustration of the relationships among R_t , reported incidence and interventions can be found in Figure 2.

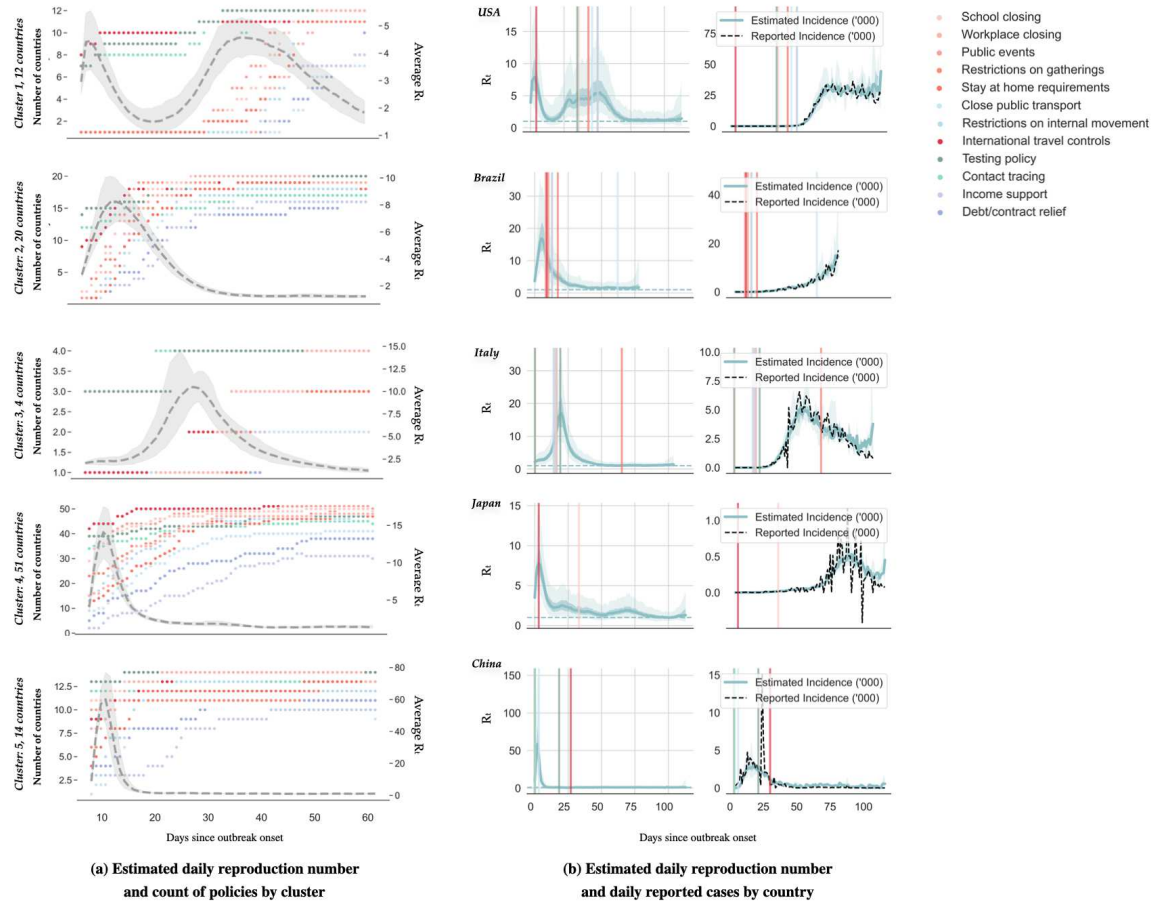
Cluster 1 has 12 countries featuring the longest duration of R_t peak. Interestingly, we observed two R_t peaks of similar levels appeared in these countries (please see Figure 2), where the first one took place during the second week since the outbreak; and the second was after 45.7 (37.08,54.25) days. This cluster includes countries such as Australia and US who started international travel control and contact tracing shortly after the initial outbreak, but delayed subsequent social distancing measures by a few weeks.

Likewise, cluster 2 reached the peak of R_t 21.8 (12.59,31.01) days from the onset, which is about 7 days later than the cluster 1. The duration of its peak is also about 3 days shorter. The 20 countries in this cluster, such as Brazil and New Zealand, adopted most interventions (7.3 (6.68,7.82)) with the shortest gap between any two interventions (7.1 (5.06,9.05) days) compared to other clusters, and they have the second lowest mortality per infection (0.04 (0.033,0.05) death/infection).

Cluster 3 contains 4 countries: Italy, Spain, Belgium and Sweden. The average level of R_t and the duration of the peak are similar to the cluster 2. However, their mortality rate is more than 3 times higher than the second cluster. This severe mortality burden has been featured in a recent study¹⁶. We saw these 4 countries are also characterized by the highest infection rates (4.1 cases per thousand population), the highest testing rates (35.7 tests per thousand population), and an aging population (20.1% of the population of these four countries aged 65 or above¹⁷). Consistent with the severe epidemic are the least number of adopted interventions (5.8) and the latest timing to apply the first social distancing policy (34.5 days) in this cluster.

Cluster 4 includes 51 countries that are similar in their transmission patterns, and cannot be distinguished under the second level of the hierarchy tree using the first 60 days of observations. The evolution of this cluster's daily R_t , including the timing and duration of its peak, is comparable to that of cluster 5 but with a much lower average and volatility. Meanwhile, this group resembles the policy adoption of cluster 2 but its R_t peak duration is shorter.

Figure 2. Patterns of early public health interventions and the evolution of effective reproduction number by cluster



a) The left panel shows the estimated daily reproduction number for each cluster during the first 60 days of the epidemics. The dashed gray line represents the median and the light gray shading represents the 5th to 95th quantiles. The number of countries that adopted the corresponding selected public health intervention are displayed using colored dots. b) The left side of the right panel shows the mean estimated daily reproduction number in selected countries until 15 May 2020. The right side of the right panel displays the reported (in dashed black line) and estimated average incidence counts (in solid blue line). In both cases, the light and dark blue shading represent 75% and 95% confidence intervals of the model estimate respectively, and the colored lines mark the initiation of the corresponding selected public health intervention.

Cluster 5 has 14 countries such as China, Iraq and Argentina. They had the highest average R_t at 4.8 (3.44,6.18), which was lifted by the R_t peak during the initial outbreak (please see Figure 2). However, their peak duration is the shortest at 3.7 (2.58,4.79) days. These countries adopted their first social intervention 7.9 (6.7,9.02) days after the outbreak which is the most prompt amongst clusters.

Overall, policy timing appeared to have a negative impact on the peak duration of R_t . For example, compare clusters 1 and 5, where the first has the longest transmission peak and the second has the shortest. This can be related to the timing of adopting social distancing measures, where cluster 5 only took one fifth of the time of cluster 1 to have around 7 policies in place. Across countries, the correlation between the number of adopted policies per unit time and the duration of the R_t peak was -0.26.

The gap between any two policies was also found to be correlated with the duration of the R_t peak, with a correlation coefficient of 0.24. Clusters 1 and 3 adopted similar number of policies with similar delays. However, the average

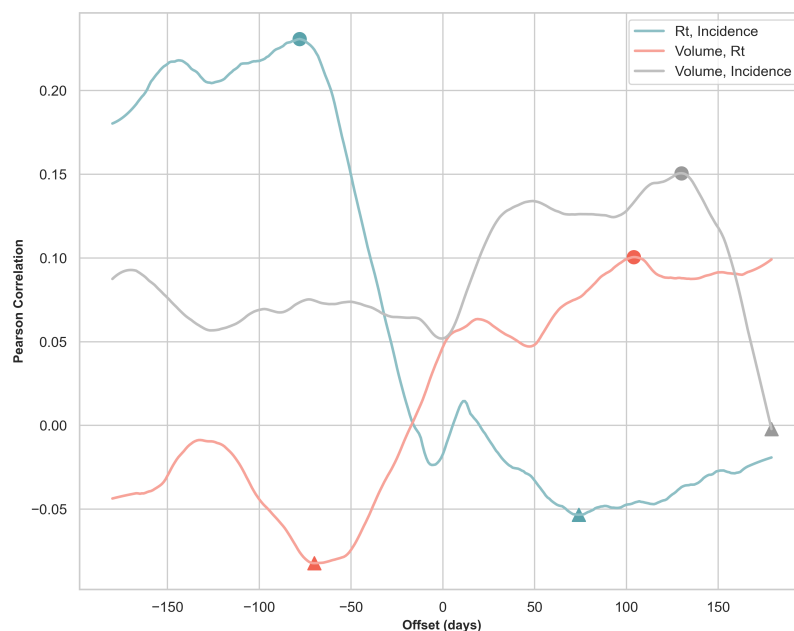
policy gap in cluster 1 was 5 days longer than in cluster 3.

There was not much difference in policy volume across clusters. By 15 May 2020, among all examined countries, on average 7.0 (6.81,7.29) social distancing measures had been adopted and around 60% of them had both testing and contact tracing policies in place. Only 32% of these countries had income support and 51% had debt or contract relief policies. The pattern of the adoption of each individual policy in these clusters is provided in the supplementary material.

The combined effect of less social distancing measures, and longer policy timing and gap can result in a prolonged peak transmission period and a higher level of R_t . By 15 May 2020, the average of median R_t across examined countries had reduced from its peak of 20.5 (17.79, 23.20) to 1.3 (0.94, 1.74).

3.2 Correlation among public health interventions, the effective reproduction number, and incidence counts

Figure 3. Time lagged cross correlation (TLCC) among selected time series



This figure depicts TLCC among selected time series for an offset from -180 days to 180 days. The solid blue line shows the TLCC between the daily effective reproduction number and the daily reported incidence count. The solid red line shows the TLCC between the daily policy volume and the daily effective reproduction number. Finally, the solid gray line shows the TLCC between the daily policy volume and the daily incidence count. All calculations are averaged over the TLCC of each country from the first count until 31 Dec 2020. The filled circles and triangles indicate the peak correlations (the maximum positive correlation or the minimum negative correlation) between two series.

The time lagged cross correlation (TLCC) among the daily effective reproduction number, the daily incidence counts, and the policy volume was estimated for each country using data since the first case detected in each country until 31 Dec 2020. Figure 3 shows the resulting correlation coefficients averaged over countries by offset days.

As it can be seen in Figure 3, the daily effective reproduction number leads the daily incidence counts by 78 days (that is when correlation is maximized). Meanwhile, the correlation between the policy volume and the daily reproduction number is two-folded. On one hand, a higher policy volume leads to lower future R_t (the negative correlation is minimized when R_t lags the policy volume by 75 days). On the other hand, a lower R_t is associated with lower future policy volume (the positive correlation is maximized when the R_t leads by 102 days). Lastly, the negative association

between the the increased policy volume and the declined incidence counts is insignificant for a lag up to 180 days. Instead, one can only observe that declined incidence counts are closely related to the lower number of policies in the future (the positive correlation is maximized when the counts lead the volume by 135 days).

Table 2. Key descriptive statistics across clusters as at 15 May 2020.

	Cluster 1 (12)	Cluster 2 (20)	Cluster 3 (4)	Cluster 4 (51)	Cluster 5 (14)
R_t , Incidence	0.34 (-76) -0.15 (63)	0.4 (-104) -0.09 (179)	0.24 (-65) -0.19 (-17)	0.21 (-149) -0.04 (74)	0.39 (-80) -0.04 (114)
Volume, R_t	0.13 (14) -0.16 (-37)	0.21 (179) -0.23 (-61)	0.17 (150) -0.29 (-67)	0.11 (103) -0.06 (-90)	0.15 (160) -0.11 (-78)
Volume, Incidence	0.17 (-105) -0.14 (-2)	0.3 (102) -0.26 (-129)	0.19 (40) -0.21 (-120)	0.16 (132) -0.01 (-179)	0.25 (168) 0.01 (-90)

This table shows the maximum positive correlation and the minimum negative correlation among the daily policy volume, the daily effective reproduction number and the daily incidence count for each cluster identified in section 3.1. We highlighted the correlation with the highest absolute value in each section and cluster. The values in the brackets record the offset days associated with the maximum or minimum correlation

In Table 2, we present the TLCC peak correlations by cluster. The first section shows that the effective reproduction number is consistently leading the incidence counts by 65 to 149 days across clusters. The second section shows how policy volume leads the effective reproduction number in clusters 1 to 3 by 37 to 67 days, while in clusters 4 and 5, higher absolute correlations are observed when policy volume leads the effective reproduction number by 103 and 160 days respectively. The last section of the table records the relationship between policy volume and incidence counts. All clusters, except from cluster 3, show significant positive correlation between the two time series. In cluster 1, a greater absolute correlation is observed when policy volume lags incidence counts by 105 days, while in clusters 2, 4 and 5 policy volume leads incidence counts by 102 to 168 days respectively.

3.3 Improved forecasting accuracy with a dynamic effective reproduction number

Forecasting of incident counts up to 30-days from the time of prediction was performed for each country. The model was able to identify 44 of the 53 countries which had a major outbreak¹ 30-days from 15 May 2020 (a true positive rate of 83.02%), as well as 38 out of 48 countries who did not experience an outbreak (a true negative rate of 79.17%).

Model predictions were reasonably stable to assumptions about the values of incubation period and the mean infectious period, although our sensitivity analysis (described in the supplementary material) observed an improvement in accuracy by assuming either a longer mean infectious period or a shorter incubation period.

Predictions were repeated over 230 daily rolling windows from 15 May 2020 until 31 Dec 2020. In a first experiment, R_t is set constant as the estimated R_t averaged over the previous 5 days. That is, when making a prediction in day 2, the model takes into account the updated reported counts, recoveries and deaths but R_t remains the same as in day 1. In a second experiment, R_t is updated dynamically every time we make a new prediction.

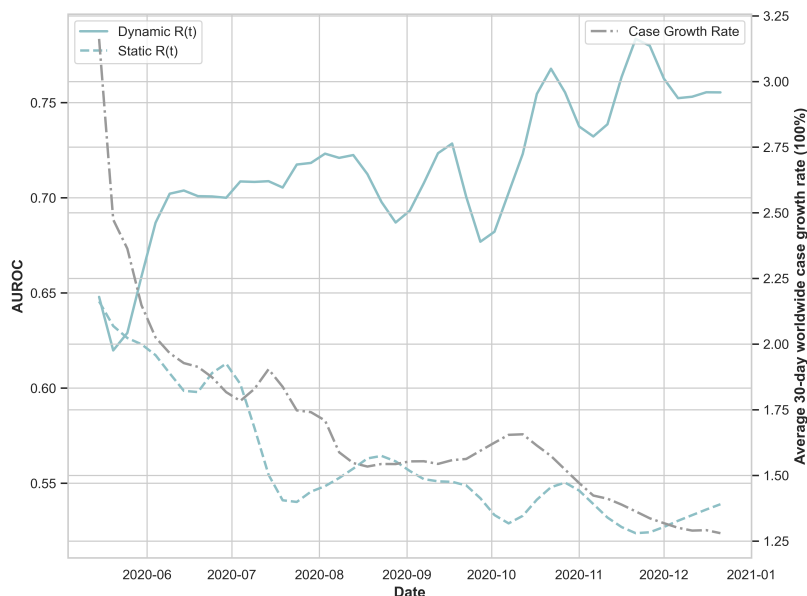
The Area under the Receiver Operating Curve (AUROC) averaged over all countries using these two methods is displayed in Figure 4. As expected the dynamic update of R_t produces more accurate results with AUROC = 0.56(0.555, 0.568) for static R_t vs. AUROC = 0.72(0.708, 0.723) for dynamic R_t .

4 Discussion

To date, various algorithms have been applied to modeling the spatial and temporal dynamics of the transmission of SARS-CoV-2, including mathematical simulation-based models^{2,4,5,7} and statistical models⁶. For example, a Wuhan

¹Defined by a growth rate threshold value $q > 1.5$, that is by the end of prediction window the cumulative counts would grow by 150% compared to the counts at the start of the window.

Figure 4. Outbreak prediction accuracy of the stochastic SEIRD model with dynamic and static effective reproduction numbers



This figure depicts the AUROC corresponding to 30-day outbreak predictions over 230 daily rolling windows from 15 May 2020 to 31 Dec 2020, and averaged over the selected 101 countries. The solid blue line corresponds to forecasts using the daily updated reproduction number averaged over the last five days previous to the time of prediction. The dashed blue line corresponds to forecasts in which the daily reproduction number remains static as the average over 11th to 15th of May 2020.

study⁴ used a deterministic, population-based compartmental model. Baseline model parameters were fitted on observed local and exported cases. The impact of containment measures was explored by assuming various contact patterns given different physical distancing scenarios. The simulation suggested sustaining intense social distancing until the end of April 2020. Similarly, an Italian study⁵ used a more complex deterministic model to analyze the effect of social distancing. Initial parameters were inferred from fitting the model outputs to observed counts, deaths and recoveries while preserving a priori information on their relative magnitude. During the course of the simulation, the effect of social distancing was modeled by changing the value of key model parameters. They found predictions were extremely sensitive to key parameters related to disease transmission, which may be a problem in the presence of changing interventions. In this case, for instance, the basic reproduction number during 29 Mar to 6 Apr 2020 (when the national lock down was fully operational) was assumed to be 0.99, compared to our estimated effective reproduction number, which varied from $R_t = 1.97(1.44, 2.50)$ to $1.07(0.76, 1.38)$ during that period. The difference between these numbers may be attributed to different model structures as well as our consideration for the lag in reporting.

The assumption of population-wide homogeneous parameters limits the ability of these deterministic models to assess the spread of disease and its decline in relation to control measures^{18,19}. During the current epidemic, a study in Singapore⁷ used agent-based influenza epidemic simulations to recreate a synthetic but realistic representation of the Singaporean population. The effect of distancing measures was then assessed by assuming different transmission rates under given social distancing policies. They recommended implementation of the quarantine of infected individuals, distancing in the workplace, and school closures immediately after having confirmed cases once international travel control has been imposed.

Further, Report 9 by Imperial College London² assigned individuals to household, school, workplace and wider community and simulated scenarios by manipulating contact rates within and between groups. They found that

a combination of case isolation, home quarantine and social distancing of aged population was the most effective scenario. This agrees with our findings that concentrated implementation of multiple interventions is most effective to contain transmission.

Rather than assessing the intervention impact via simulation, statistical models aim to represent the empirical association between public health interventions and transmission rates and/or counts. For example, Report 13 by Imperial College London⁶ used a semi-mechanistic Bayesian hierarchical model to infer the impact of social distancing and travel lock downs on the daily reproduction number in 11 European countries². The daily reproduction number was modeled as a function of the baseline reproduction number before any intervention together with multiplicative relative percent reductions in R_t from interventions. Model parameters were fitted to observed deaths in these countries as a function of the number of infections. This model had heavy assumptions on prior distributions of model parameters and assumed consistent intervention impact across countries to leverage more data for fitting. By 28 Mar 2020, they found R_t was reduced to around 1 across the 11 countries. Our study found similar reduction in R_t , which was sustained after one and a half months at 15 May 2020, when the average of the median of R_t was 1.17 (0.91, 1.53) across these countries.

Our results highlight the importance of using real-time estimates of R_t in these types of studies, since it is difficult to set epidemiological parameters under uncertain impact from public health interventions. This is particularly important given that prediction of future counts is very sensitive to simulation parameters. In this study, we demonstrated that updating the daily effective reproduction number facilitates more accurate simulations of future incidence counts as well as real-time monitoring of the effect of public health interventions.

We first conducted a hierarchical clustering analysis of R_t from 29 Jan to 15 May 2020 in order to systematically characterize early public health interventions in relation to the patterns of disease transmission across countries. The analysis revealed significant heterogeneity in the effect of control measures on the daily effective reproduction number. For example, there were two transmission peaks in countries such as Australia and the US, which started international travel control shortly after the onset, but delayed subsequent social distancing measures by a few weeks. The clustering analysis also questioned the effect of testing and contact tracing in the presence of community transmission and in the absence of social distancing. Italy, Spain, Belgium and Sweden were among the top 8 countries with the highest mortality burden¹⁶ and they were also among the top 10 countries carrying out most tests per population.

This heterogeneous effect makes it challenging to forecast future outbreaks by looking solely at the current interventions and disease counts. In fact, our time lagged cross correlation analysis revealed that the negative correlation between the number of implemented policies and the level of virus transmission is reflected only in the updated daily effective reproduction number but not in the incidence counts up to a lag of 180 days due to the substantial delay between the policy implementation and the reduction in incidence counts. Therefore, the calculated R_t keeps a much closer track of the prevailing disease transmission trend than the reported incidence counts, and using updated R_t in conventional SEIRD simulations can improve the predictions on future outbreaks.

Using the estimated daily effective reproduction number, we are able to forecast future outbreaks with reasonable accuracy from 15 May to the end of 2020. In particular, we predicted the worrisome increase in outbreak probability in countries like South Africa, Chile and Brazil in June 2020 and the possibility of second outbreaks in countries like UK, USA, France, Germany, Portugal, Italy and Japan in Nov 2020.

4.1 Limitations

There are several limitations to our analysis. The estimated daily reproduction number is specific to our extended, population-level SEIRD model. This model does not represent the heterogeneity of transmission within a country, and therefore, may be less relevant for countries such as the US and China, which have varied adoption of interventions across regions. Researchers using other models need to estimate their own transmission parameters in a similar manner.

²11 countries in the original study are Austria, Belgium, Switzerland, Germany, Denmark, Spain, France, United Kingdom, Italy, Norway and Sweden.

Our stochastic model does not fit well during the initial week of the epidemic outbreak, when only a small number of data points were available across countries. Over time, the availability and reliability of data improved, which was reflected in an increased model prediction accuracy, where the absolute bias of fitted daily incidents is below 15% (please refer to the supplementary material for more details). Nevertheless, we acknowledge that varied data quality across countries may influence the accuracy of our analyses. In particular, WHO’s daily Situation Reports shifted its reporting cutoff time on 18 Mar 2020, which compromised the comparability of its earlier figures. There was not much difference between the other two sources of disease counts²⁰ except that Johns Hopkins also included estimates of presumptive positive cases that have been confirmed by state or local labs, but not by national labs. Two well-known problems of SARS-CoV-2 data are under-reporting of cases and delays in reporting. We attempted to account for both problems by introducing a parameter representing the proportion of actual cases detected via testing, as well as a delay in reporting. We used plausible biological parameters for SARS-CoV-2 based on current evidence, but these values might be refined as more clinical evidence becomes available. The standardized intervention measures from Oxford Covid-19 Government Response Tracker, may also suffer from inaccuracies. As the updating frequency of the tracker is performed once a week in most countries, we infer the days with missing policy using the last observed policy in that country.

4.2 Conclusions

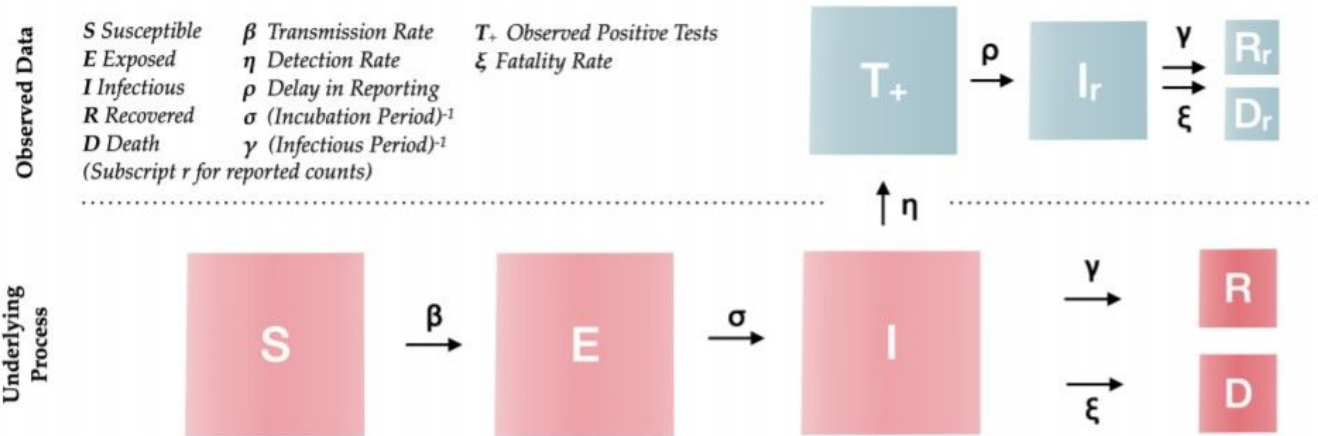
This study provides an estimate of the daily effective reproduction number of the transmission of the SARS-CoV-2 virus across countries over time as various public health interventions were adopted. This allows us to look at the evolution of disease transmission in the presence of containment measures. We confirmed the importance of using updated reproduction numbers for the monitoring of future outbreaks.

- [1] World Health Organization. Rolling updates on coronavirus disease (covid-19) (updated 31 July 2020), 2020.
- [2] Neil Ferguson, Daniel Laydon, Gemma Nedjati Gilani, Natsuko Imai, Kylie Ainslie, Marc Baguelin, Sangeeta Bhatia, Adhiratha Boonyasiri, ZULMA Cucunuba Perez, Gina Cuomo-Dannenburg, et al. Report 9: Impact of non-pharmaceutical interventions (npis) to reduce covid19 mortality and healthcare demand. 2020.
- [3] Stephen A Lauer, Kyra H Grantz, Qifang Bi, Forrest K Jones, Qulu Zheng, Hannah R Meredith, Andrew S Azman, Nicholas G Reich, and Justin Lessler. The incubation period of coronavirus disease 2019 (COVID-19) from publicly reported confirmed cases: estimation and application. *Annals of internal medicine*, 172(9):577–582, 2020.
- [4] Kiesha Prem, Yang Liu, Timothy W Russell, Adam J Kucharski, Rosalind M Eggo, Nicholas Davies, Stefan Flasche, Samuel Clifford, Carl AB Pearson, and James D Munday. The effect of control strategies to reduce social mixing on outcomes of the covid-19 epidemic in wuhan, china: a modelling study. *The Lancet Public Health*, 2020.
- [5] Giulia Giordano, Franco Blanchini, Raffaele Bruno, Patrizio Colaneri, Alessandro Di Filippo, Angela Di Matteo, and Marta Colaneri. Modelling the COVID-19 epidemic and implementation of population-wide interventions in Italy. *Nature Medicine*, 26(6):855–860, 2020.
- [6] Seth Flaxman, Swapnil Mishra, Axel Gandy, H Unwin, Helen Coupland, T Mellan, Harisson Zhu, T Berah, J Eaton, and P Perez Guzman. Report 13: Estimating the number of infections and the impact of non-pharmaceutical interventions on covid-19 in 11 european countries. 2020.
- [7] Joel R Koo, Alex R Cook, Minah Park, Yinxiaohe Sun, Haoyang Sun, Jue Tao Lim, Clarence Tam, and Borame L Dickens. Interventions to mitigate early spread of SARS-CoV-2 in Singapore: a modelling study. *The Lancet Infectious Diseases*, 2020.
- [8] Thomas Hale and Samuel Webster. Oxford covid-19 government response tracker, 2020.
- [9] Joseph Dureau, Konstantinos Kalogeropoulos, and Marc Baguelin. Capturing the time-varying drivers of an epidemic using stochastic dynamical systems. *Biostatistics*, 14(3):541–555, 2013.
- [10] Ensheng Dong, Hongru Du, and Lauren Gardner. An interactive web-based dashboard to track covid-19 in real time, 2020.
- [11] M Kramer, D Pigott, B Xu, S Hill, B Gutierrez, and O Pybus. Epidemiological data from the ncov-2019 outbreak: early descriptions from publicly available data, 2020.
- [12] Tao Liu, Jianxiong Hu, Min Kang, Lifeng Lin, Haojie Zhong, Jianpeng Xiao, Guan hao He, Tie Song, Qiong Huang, and Zuhua Rong. Transmission dynamics of 2019 novel coronavirus (2019-ncov). 2020.
- [13] Qun Li, Xuhua Guan, Peng Wu, Xiaoye Wang, Lei Zhou, Yeqing Tong, Ruiqi Ren, Kathy SM Leung, Eric HY Lau, and Jessica Y Wong. Early transmission dynamics in wuhan, china, of novel coronavirus-infected pneumonia. *New England Journal of Medicine*, 2020.
- [14] Abraham Savitzky and Marcel JE Golay. Smoothing and differentiation of data by simplified least squares procedures. *Analytical chemistry*, 36(8):1627–1639, 1964.
- [15] Tom Fawcett. An introduction to ROC analysis. *Pattern recognition letters*, 27(8):861–874, 2006.
- [16] Philip Schellekens and Diego M Sourrouille. Covid-19 mortality in rich and poor countries: a tale of two pandemics? *World Bank Policy Research Working Paper*, (9260), 2020.
- [17] The UNESCO Institute for Statistics (UIS). Demographic and socio-economic statistics, 2020.
- [18] Chris Dye and Nigel Gay. Modeling the sars epidemic. *Science*, 300(5627):1884–1885, 2003.
- [19] Alison P Galvani. Emerging infections: what have we learned from sars? *Emerging infectious diseases*, 10(7):1351, 2004.
- [20] Our World in Data. Covid-19 deaths and cases: how do sources compare?, 2020.

Contributions

J.Z and B.G. suggested the design. J.Z. conducted the simulations. J.Z and B.G. collected the results. J.Z prepare the figures. J.Z and B.G. wrote the main text. All authors reviewed the manuscript.

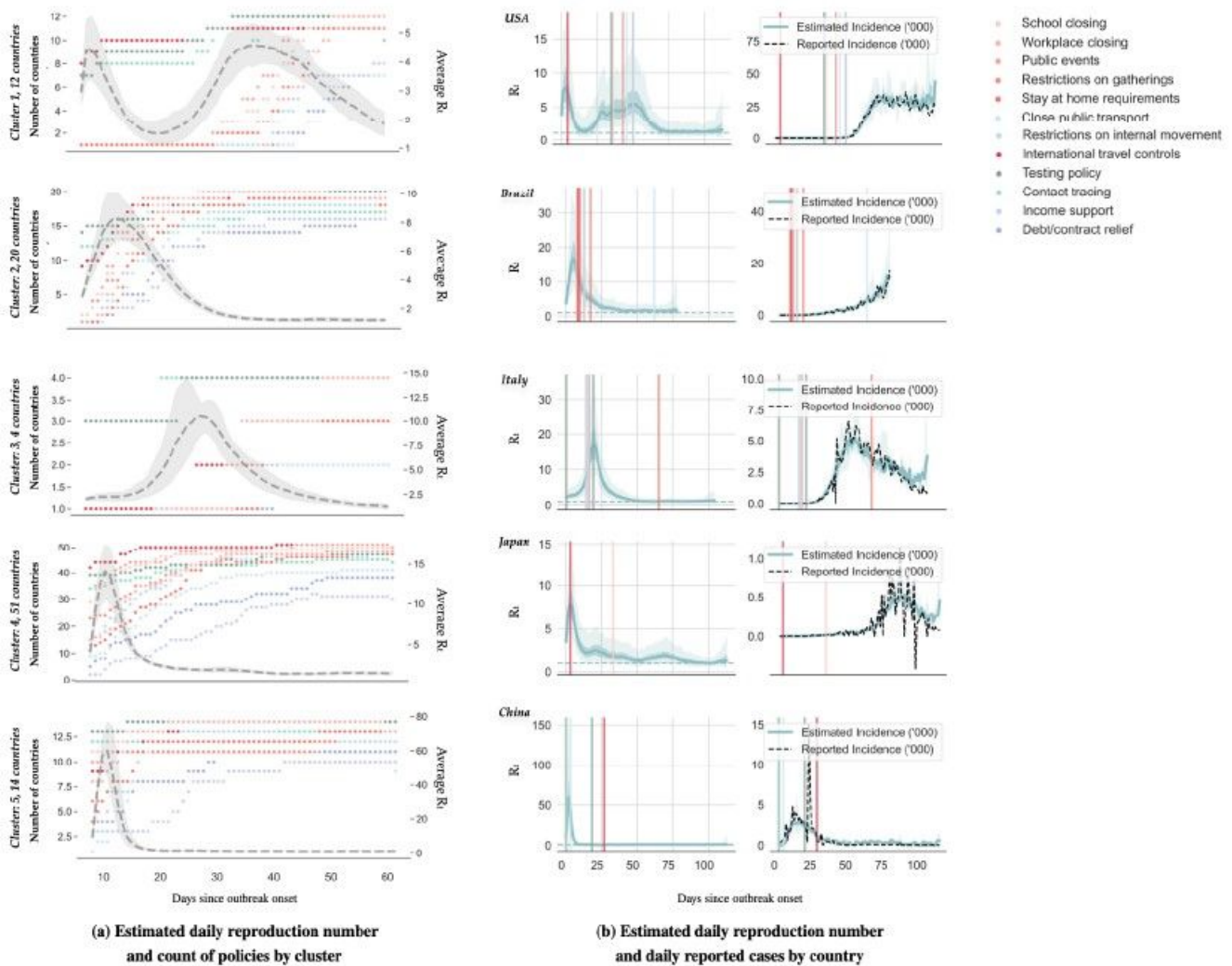
Figures



The population is divided into the following five classes: susceptible, exposed (non-infectious and asymptomatic), infectious (asymptomatic and symptomatic), removed (i.e., isolated, recovered, or otherwise non-infectious) and dead. The reported data is modeled with four classes: observed positive tests, reported infections, removed and deaths.

Figure 1

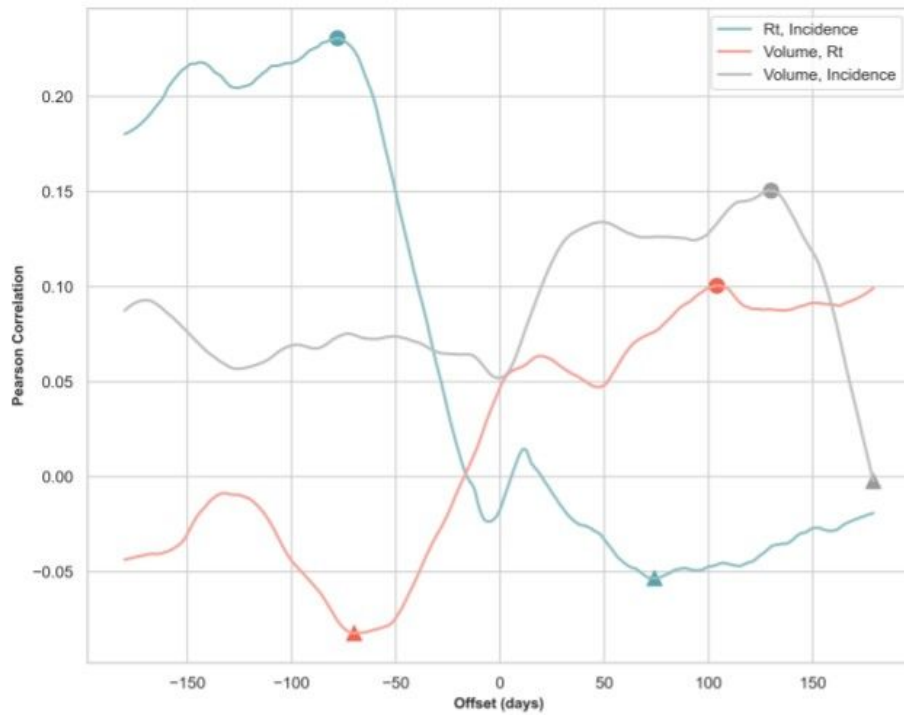
Simulation model structure.



a) The left panel shows the estimated daily reproduction number for each cluster during the first 60 days of the epidemics. The dashed gray line represents the median and the light gray shading represents the 5th to 95th quantiles. The number of countries that adopted the corresponding selected public health intervention are displayed using colored dots. b) The left side of the right panel shows the mean estimated daily reproduction number in selected countries until 15 May 2020. The right side of the right panel displays the reported (in dashed black line) and estimated average incidence counts (in solid blue line). In both cases, the light and dark blue shading represent 75% and 95% confidence intervals of the model estimate respectively, and the colored lines mark the initiation of the corresponding selected public health intervention.

Figure 2

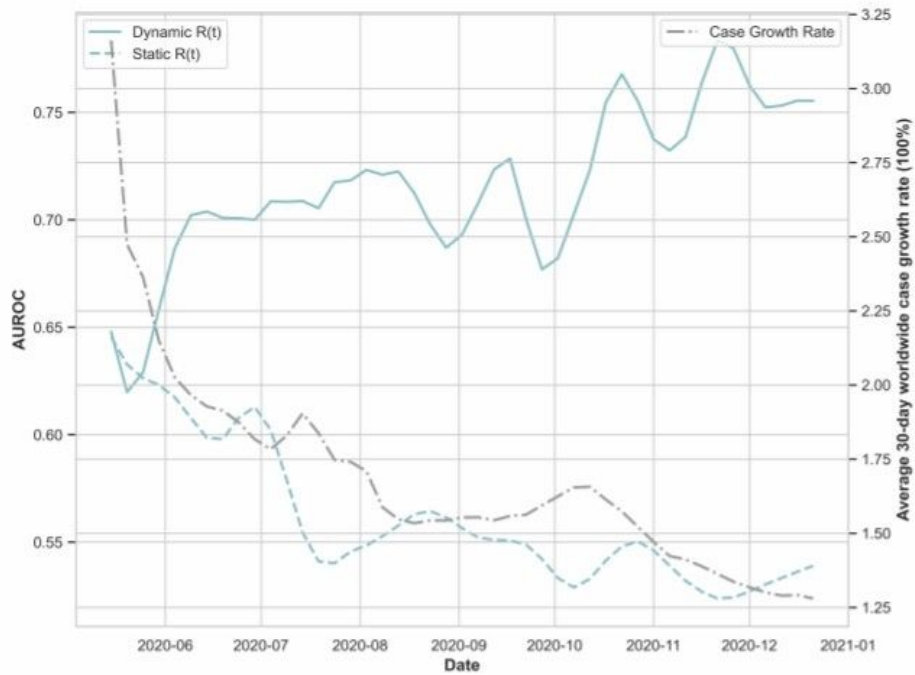
Patterns of early public health interventions and the evolution of effective reproduction number by cluster



This figure depicts TLCC among selected time series for an offset from -180 days to 180 days. The solid blue line shows the TLCC between the daily effective reproduction number and the daily reported incidence count. The solid red line shows the TLCC between the daily policy volume and the daily effective reproduction number. Finally, the solid gray line shows the TLCC between the daily policy volume and the daily incidence count. All calculations are averaged over the TLCC of each country from the first count until 31 Dec 2020. The filled circles and triangles indicate the peak correlations (the maximum positive correlation or the minimum negative correlation) between two series.

Figure 3

Time lagged cross correlation (TLCC) among selected time series



This figure depicts the AUROC corresponding to 30-day outbreak predictions over 230 daily rolling windows from 15 May 2020 to 31 Dec 2020, and averaged over the selected 101 countries. The solid blue line corresponds to forecasts using the daily updated reproduction number averaged over the last five days previous to the time of prediction. The dashed blue line corresponds to forecasts in which the daily reproduction number remains static as the average over 11th to 15th of May 2020.

Figure 4

Outbreak prediction accuracy of the stochastic SEIRD model with dynamic and static effective reproduction numbers